DIGITAL SIMULATION OF HYDRAULIC POSITIONAL SERVOMECHANISM CONSIDERING THE HYSTERESIS BACKLASH AND THE HYDRAULIC FLUID COMPRESSIBILITY

TRAN VAN DAC

Department of Precision-Mechanics and Applied Optics,
Technical University, H-1521 Budapest

Received April 11, 1985
Presented by Prof. Dr. O. Petrik

Abstract

In hydraulic positional servomechanism the hydraulic fluid compressibility variation due to air bubbles, namely the increase of air volume ratio in oil gives rise to a negative fact in the behavior of the system. The presence of hysteresis backlash brings about the limit cycle in the second-order system, but for a third-order system the backlash ameliorates the condition of system stability, in spite of controlling accuracy. Besides, in this case limit cycle does not occur.

The present paper deals with the above problems and gives some interesting conclusions which can be used in engineering practice.

Introduction

Until now the investigation of hydraulic positional mechanism has usually been based upon the linear model. These systems are strongly nonlinear because, on the one hand the hydrodynamic processes are very complicated, on the other hand Coulomb's friction and backlash in addition, commonly make for a new multy-valued nonlinearity. By means of the usual method the investigation of such systems is very tiring and long. But nowadays, modern calculation technique as an effectual means gives a lot of aid to engineers in their activity.

The present paper endeavours to investigate theoretically a copying shaper having two-control edge valve as regards hysteresis backlash and hydraulic fluid compressibility, in a manner by extending the usual linear model [3] by the mentioned nonlinearity. The obtained result coincides with the one in [1]. But it is sure that this simulation gives a more exact result than the isocline method for the second-order system, and it is the only way which may give a result for the third-order system when the compressibility of hydraulic fluid is not negligible. The computer program may be used for an investigation of a similar system having discretional parameters.

The modelling of the system

In the following control system often the hysteresis backlash is due to the gear-drive and linkage in the mechanical part of the system if we consider these to be totally stiff and Coulomb's friction to be present. They make a nonlinearity as a feedback element of the controlled system depending on what we consider the system controlled variable. In the present case, for the mentioned system, this nonlinearity is the feedback element (see Fig. 1). It is

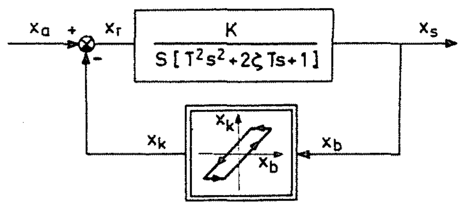

Fig. 1. Block diagram of the system

interesting to remember that the transfer function of the linear element may be written in an other form [2], however in such a case its constants have a different physical sense. But in point of view of the solution the results are the same. In Fig. 1 the senses of the designation are

x_a = command signal or system input signal
x_r = system error signal or actuating signal
x_b, x_k = input and output signal of the nonlinearity, respectively
x_s = controlled signal or system output signal
s = Laplace transform variable
T and ζ = time constant and damping ratio of the linear element, respectively
K = the open loop gain.

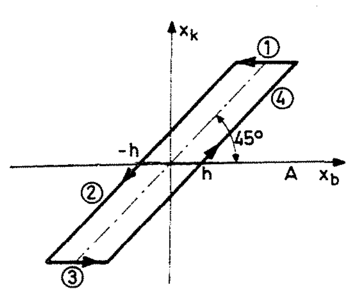

Fig. 2. Characteristics of the hysteresis blacklash

Let us consider in detail the nonlinear element. Basically this element is a typical nonlinearity which is linear zone by zone, i.e., it is the piecewise linear element due to the effect of Coulomb's friction and backlash (or the dead zone). With the designation of Fig. 2 between the input x_b and the output x_k of the nonlinearity we find the following relations:
for piece 1

$$x_k = A - h = \text{const.} \tag{1a}$$

for piece 2

$$x_k = x_b + h \tag{1b}$$

for piece 3

$$x_k = -A + h = \text{const.} \tag{1c}$$

and for piece 4

$$x_k = x_b - h \tag{1d}$$

where

A = time amplitude of input signal of the nonlinearity.

For the sake of the system consideration let the system input signal (i.e., x_a) be Dirac's impulse, i.e., $x_a(t) = \delta(t)$. In accordance with Fig. 1 and Eqs (1a)–(1d) one may obtain the following differential equations

$$\left.\begin{aligned} T^2\dddot{x}_s + 2\zeta T\ddot{x}_s + \dot{x}_s + K(A-h) &= 0 \\ T^2\dddot{x}_s + 2\zeta T\ddot{x}_s + \dot{x}_s + K(x_s+h) &= 0 \\ T^2\dddot{x}_s + 2\zeta T\ddot{x}_s + \dot{x}_s + K(-A+h) &= 0 \\ T^2\dddot{x}_s + 2\zeta T\ddot{x}_s + \dot{x}_s + K(x_s-h) &= 0 \end{aligned}\right\} \tag{2}$$

respectively.

If the system input signal is the step function $x_a(t) = X_a 1(t)$ then by variable transformation $x_s^*(t) = x_s(t) - KX_a$ the form of the corresponding equations is similar to the one of (2). Therefore in this case the solution procedure is also similar. By an inverse transformation the time dependent response may be received. For the solution procedure it is sufficient to deal with case (2).

It is well known that in case of a hydraulic servomechanism, if the hydraulic fluid compressibility is negligible, the transfer function of the linear element may be written in the following form [3]

$$Y(s) = \frac{K}{s(Ts+1)} \tag{3}$$

In this case the corresponding describing differential equations are

$$\left.\begin{aligned} T\ddot{x}_x+\dot{x}_s+K(A-h)=0 \\ T\ddot{x}_s+\dot{x}_s+K(x_s+h)=0 \\ T\ddot{x}_s+\dot{x}_s+K(-A+h)=0 \\ T\ddot{x}_s+\dot{x}_s+K(x_s-h)=0 \end{aligned}\right\} \quad (4)$$

also for the system input signal $x_a(t)=\delta(t)$ (i.e., Dirac's impulse).

In principle Eqs. (3) or (4) may be solved by the customary method well known in the domain of ordinary differential equations considering the property of the piecewise linear. Thus the initial condition of integration curve in the next zone is the value of the final point of the integration curve in the preceding one. So, step by step we may determine a total integration curve for a given initial codition. It is easily seen this method is time consuming and complicated. With a more comfortable procedure, the isocline method can be used to solve the problem, but the necessary accuracy is not assured.

For the purpose of a more exact and clear solution we shall use the phase-space method for both (2) and (4), with the trajectories drawn in the isometrical axonometric coordinate system. The dashed curves indicate phase points where the acceleration $\ddot{x}_s(t)$ is negative.

In the following we shall use a numerical method, the fourth-order Runge-Kutta algorithm. This is one of the most accurate methods of numerical analysis.

Illustrative example

Here we used the data of the example in [4], for a copying shaper, namely:
system operation pressure $p_0=20$ bar $\approx 2\cdot 10^6$ N/m^2
the larger and the smaller surface of the actuator piston

$$A_{10}=4\cdot 10^{-3}\ \text{m}^2 \text{ and } A_0=2\cdot 10^{-3}\ \text{m}^2$$

the flow factor of the controlling valve $\mu=0.75$
specific weight of pure oil $\gamma_0=8000$ N/m^3
reduced mass of moving elements $m=2$ kg
the largest volume capacity of the actuator cylinder

$$V=2.4\cdot 10^{-4}\ \text{m}^3$$

the compressibility modulus of pure oil $\beta_0=5\cdot 10^{-8}$ m^2/N
fluid friction factor $B=1000$ Ns/m
nominal diameter of the controlling valve $d=1.8\cdot 10^{-2}$ m

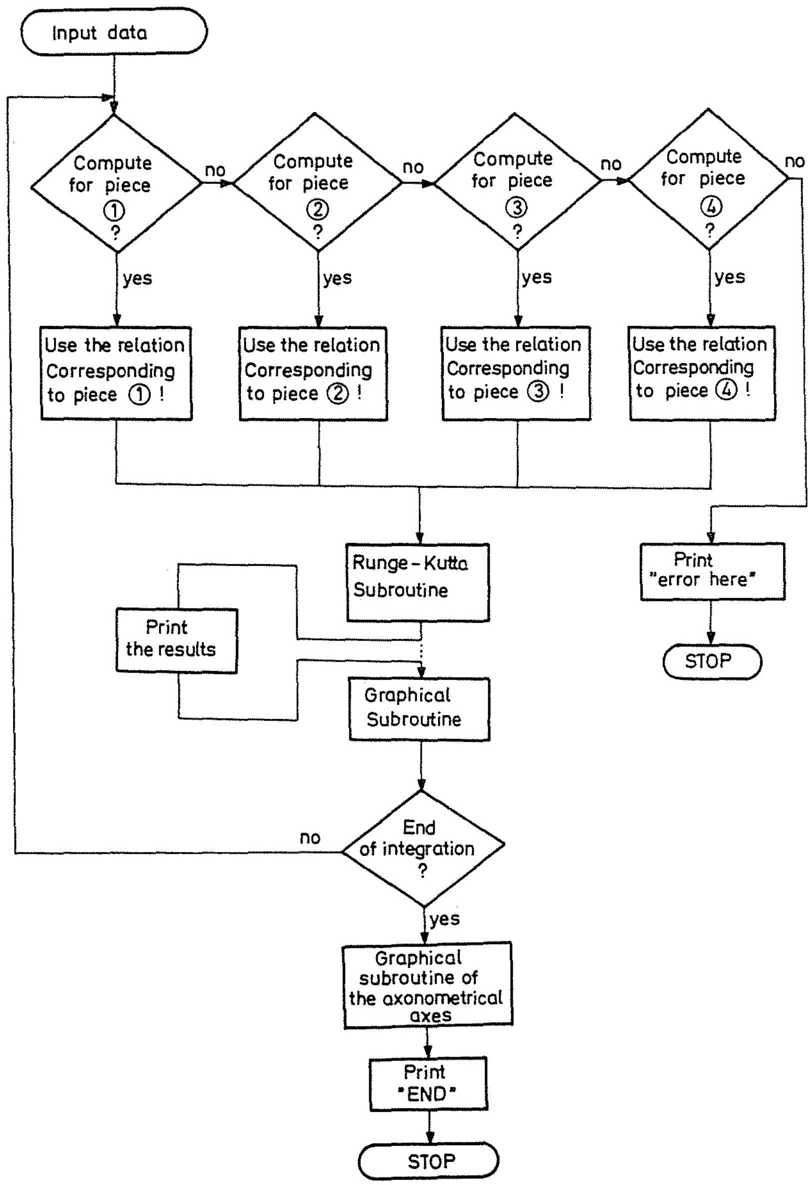

Fig. 3. The program flowchart

the negative overlap of the controlling valve

$$\varepsilon_0 = 10^{-4}\ \text{m} \quad (=100\ \mu\text{m})$$

the force amplification factor $B_0 = 8 \cdot 10^3$ N/m
the speed amplification factor $D_0 = 10^3$ 1/s
After these we may receive the following tabulated result (see Tab. 1), where

v = volume ratio of air-oil mixture
T_2 = system time constant
ζ = system damping ratio
K = open loop gain.

Table 1

v %	$T_2 \cdot 10^4$ s	2ζ	K
0.00	3.850	0.660744	987.65
0.20	4.037	0.632414	988.63
0.40	4.217	0.607724	989.61
0.60	4.391	0.585964	990.59
0.80	4.558	0.566610	991.57
1.00	4.720	0.549256	992.56
1.20	4.878	0.533588	993.35
1.40	5.031	0.519356	994.55
1.48	5.091	0.514042	994.95
1.60	5.180	0.506358	995.55
1.80	5.325	0.494430	996.55
2.00	5.467	0.485438	997.55

It is also to be noticed, that to receive the results in Tab. 1 we used the following expressions [4]:

$$T_2 = \left\{ \frac{1 + (E_0/p_0^2)v/(1-v)\beta_0}{\left(\dfrac{BK_{Q_0}}{1-v} + 4A_0^2K_p\right)\left(1 + \dfrac{v}{p_0(1-v)}\right)} \right\}^{1/2}$$

where

K_p = the pressure difference amplification factor
K_{Q_0} = the volume flow amplification factor (for pure oil)
E_0 = $1/\beta_0$

$$\zeta = \frac{1}{2T_2} \cdot \frac{mK_{Q_0}/\sqrt{1-v} + VK_pB\beta}{BK_{Q_0}/\sqrt{1-v} + 4A_0^2K_p}$$

$$\beta = \frac{1 + p_a v/p_0^2(1-v)}{1 + p_a v/p_0(1-v)}\beta_0$$

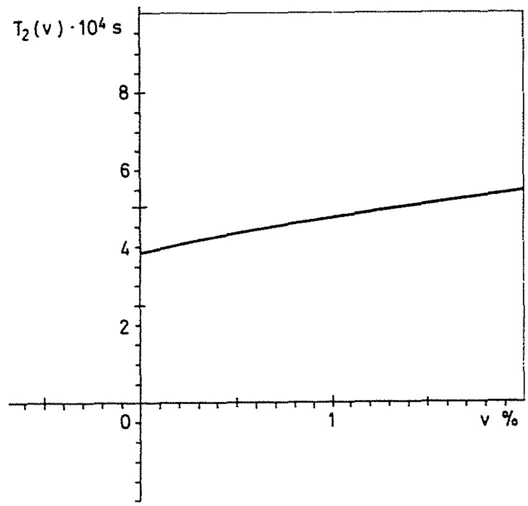

Fig. 4. Diagram of function $T(v)$

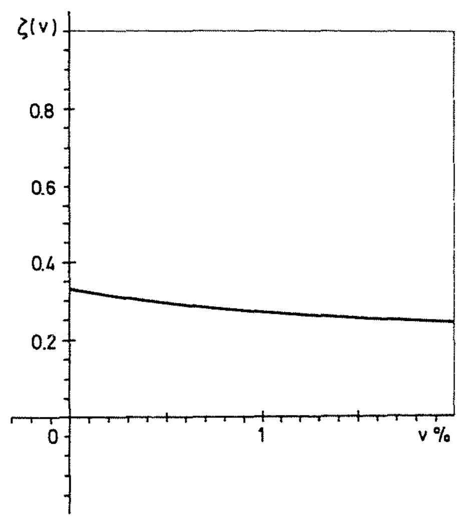

Fig. 5. Diagram of function $\zeta(v)$

and

$$K = \frac{2A_0K_pK_{Q0}/\sqrt{1-v}}{BK_{Q0}/\sqrt{1-v}+4A_0^2K_p}$$

When the compressibility of the hydraulic fluid is negligible the value of the system parameters (i.e., the open loop gain K and the time constant T_2) are:

$$K = 957$$

and

$$T_2 = 2.39 \cdot 10^{-4}\, s\,.$$

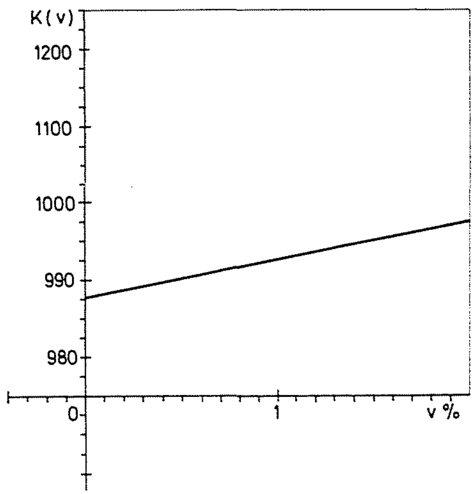

Fig. 6. Diagram of function $K(v)$

Using these values it may be stated what the system behavior is like at different magnitudes of backlash. Especially the question has to be answered if there is a limit cycle or the limit cycle in system operation may be proven. In addition we may determine the relation between the backlash magnitude and the limit cycle amplitude.

When the hydraulic fluid compressibility is not negligible we also have answer to questions similar to the ones mentioned above and as we shall see later, for the system behaviour we discovered a lot of interesting properties.

In the following we first deal with the case of incompressibility, and then that of compressibility. All results are summarized in tables and diagrams.

If the fluid compressibility is negligible, it follows that the system characteristic polynomial (i.e., the denominator of the transfer function) is second-order. In this case the open loop gain and the time constant are invariable. The model has only one variable parameter, the backlash magnitude. Nevertheless when the fluid compressibility changes due to the presence of air bubbles, besides the backlash parameter there is also an other parameter, the air-oil volume ratio v, which changes the open loop gain, the time constant and the damping ratio. Since the variation speed of the latter are very much smaller (by several orders) than the frequency of the system, we consider these not to be system variables, they are system parameters (see Figs 4, 5 and 6 and Tab. 1).

a) *Case of incompressibility* (the second-order system). The results of this case are summarized in Tables 2 and 3, and Figs 7, 8, 9 and 10.

We see that in this case a limit cycle exists.

b) *Case of compressibility* (the third-order system). It must be kept in mind

Table 2

Values of function $x(t)$, $y(t)$ and $z(t)$

Time $10^6 \cdot t$ [s]	Displacement x [μm]	Speed y [m/s]	Acceleration $10^{-7} \cdot z$ [m/s^2]
0.0	4818.0	0.0	0.00
10.0	1316.5	−600.4	−2.2234257
20.0	−4091.4	−327.3	6.7715374
34.4	−1276.8	601.9	2.1564891
44.4	4112.9	322.8	−6.8055412
58.7	1297.2	−601.1	−2.1908126
68.7	−4102.0	−325.1	6.7888670
83.1	−1257.5	602.5	2.1239103
93.1	4123.4	320.6	−6.8235381
107.4	1277.9	−601.8	−2.1583076
117.4	−4112.5	−322.9	6.8059564
131.7	−1298.3	601.1	2.1926224
141.7	4101.6	325.2	−.67882650
156.1	1258.5	−602.5	−2.1257074
166.1	−4123.0	−320.7	6.8229453
180.4	−1279.0	601.8	2.1600913
190.4	4112.2	323.0	−6.8053514
204.7	1299.3	−601.1	−2.1943982
214.7	−4101.3	−325.3	6.7876440
229.1	−1259.6	602.5	2.1274716
239.1	4122.6	320.8	−6.8223340
253.4	1280.0	−601.8	−2.1618427
263.4	−4411.8	−323.1	6.8047290
277.7	−1300.4	601.1	2.1961424
287.7	4100.9	325.5	−6.7870068
302.1	1260.6	−602.5	−2.1292053
312.1	−4122.2	−321.0	6.8217070
326.4	−1281.0	601.8	2.1635644
336.4	4111.4	323.3	−6.8040919
350.7	1301.4	−601.1	−2.1978573

Table 3

Relation between backlash and limit cycle amplitude

The backlash magnitude h [μm]	The limit cycle amplitude $A_{hc} = x_{sh}$ [μm]
10	48.19
20	96.39
40	192.79
60	289.23
80	386.15
100	481.39
120	579.02
140	675.24
160	771.71

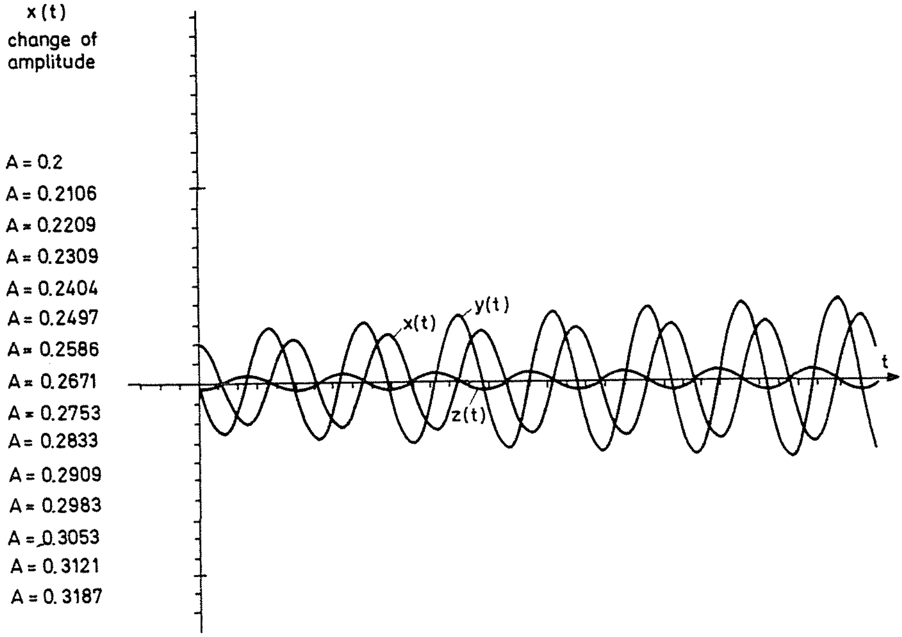

Fig. 7a. Diagram of functions $x(t)$, $y(t)$, $z(t)$ (tending from inside to the limit cycle)

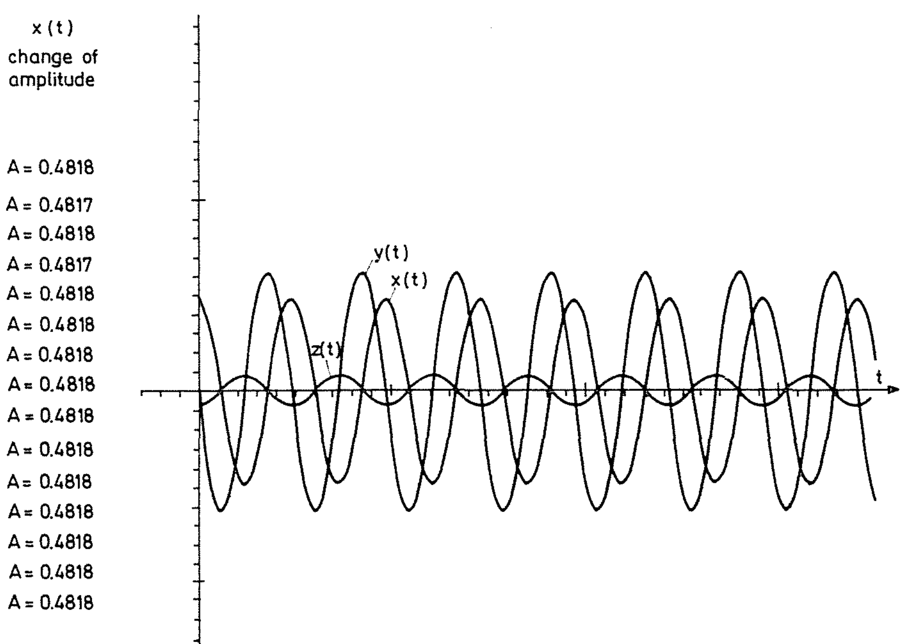

Fig. 7b. Diagram of functions $x(t)$, $y(t)$, $z(t)$ (for the limit cycle case)

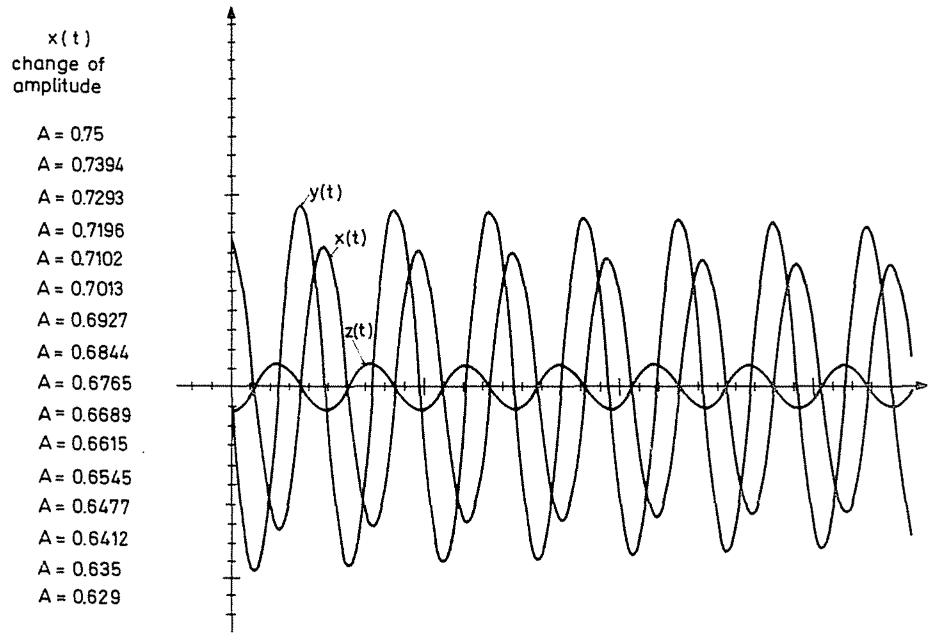

Fig. 7c. Diagram of functions $x(t)$, $y(t)$, $z(t)$ (tending from outside to the limit cycle)

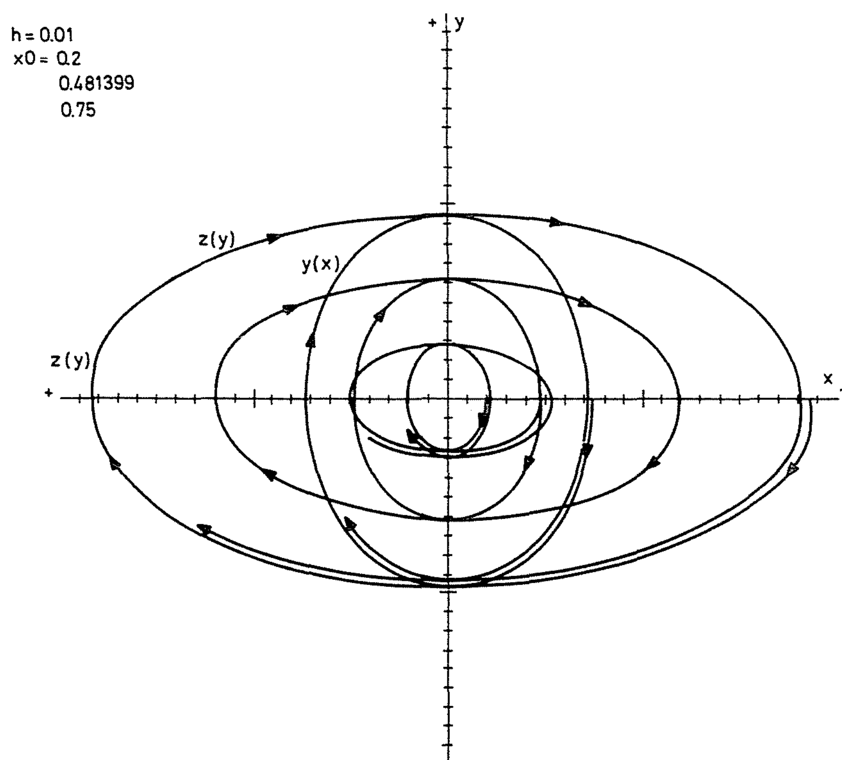

Fig. 8. Projection of the spatial trajectories (i.e., diagram of function $y(x)$, $z(y)$)

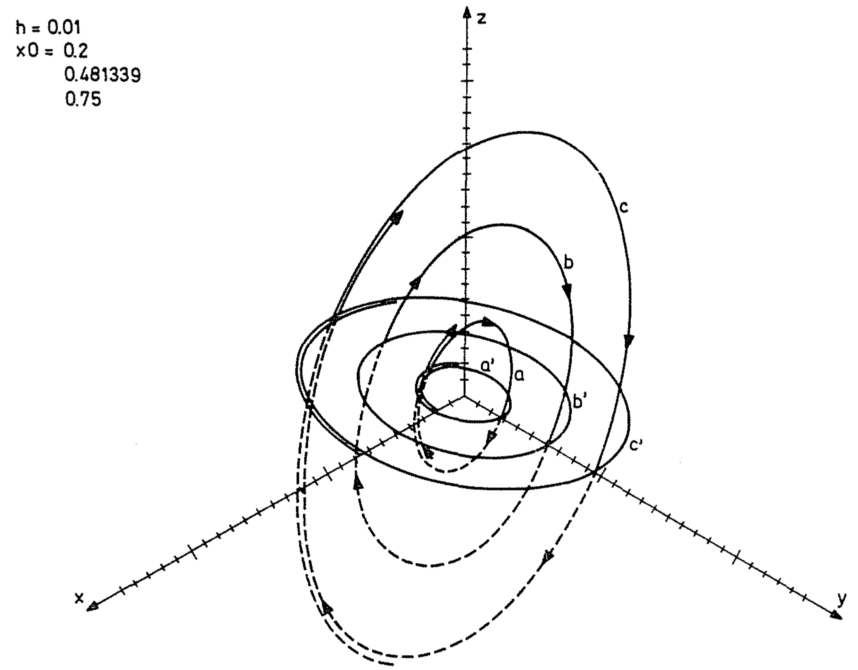

Fig. 9. Spatial trajectories a, a′: trajectory and its projection in (x, y) plain, which tends from inside to the limit cycle; b, b′: trajectory and its projection in (x, y) plain for the limit cycle; c, c′: trajectory and its projection in (x, y) plain which tends from outside to the limit cycle

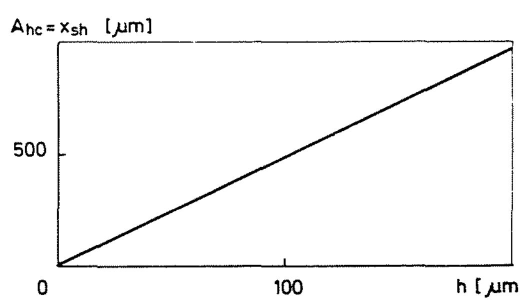

Fig. 10. Relation between backlash and limit cycle amplitude

that at every v value greater than 1.48% (i.e., $v = 0.0148$) the system in question is instable, if it is backlash free, [3] as seen in Fig. 11. The results of this case are also summarized in Tabs. 4, 5, 6 and Figs 11, 12, 13, 14 and 15.

Table 4

Values of function $x(t)$, $y(t)$ and $z(t)$

Time $10^3 \cdot t$ [s]	Displacement x [μm]	Speed $10^{-2} \cdot y$ [m/s]	Acceleration z [m/s²]
0.00	110.11	0.0000	0.00
0.50	104.68	− 3.0546	−105.60
1.00	75.13	− 8.7711	−106.81
1.50	20.81	−12.1479	− 10.94
2.00	− 35.24	− 9.0803	130.30
2.50	− 60.47	− 0.4894	191.60
3.00	− 38.38	8.1149	113.55
3.50	11.13	10.5661	− 21.92
4.00	55.13	5.9211	−153.39
4.50	59.67	− 4.4960	−163.33
5.12	− 20.63	−10.2290	− 57.60
5.62	− 31.81	− 9.5196	87.96
6.12	− 63.40	− 2.3246	181.45
6.50	− 59.07	4.4876	163.71
7.00	− 20.05	10.2191	57.04
7.50	32.26	9.4746	− 88.66
8.00	63.56	2.2583	−181.52
8.63	43.37	− 8.0148	−117.05
9.13	− 6.32	−10.7810	13.85
9.88	− 63.51	− 2.2951	181.42
10.50	− 43.52	7.9917	117.49
11.00	6.12	10.7837	− 13.26
11.50	52.23	6.5186	−148.26
12.13	59.16	− 4.4802	−163.76
12.63	20.16	−10.2184	− 57.24
13.13	− 3.21	− 9.4850	88.45
13.63	− 63.54	− 2.2747	181.50
14.51	− 20.36	10.2078	57.74
15.01	31.99	9.5025	− 87.92
15.51	63.50	2.3098	−181.39
16.14	43.19	− 8.0421	−116.58
16.64	− 6.57	−10.7795	14.54
17.14	− 52.51	− 6.4569	149.10
17.76	− 59.21	4.4682	163.89

Table 5

Relation between backlash and initial controlled signal (*at* $v = 2\%$)

h [μm]	x_0 [μm]
0	0.0
5	27.5
10	55.0
15	82.6
20	110.1

Table 6

Relation between backlash and critical oscillation amplitude (at $v = 2\%$)

h [μm]	A_h [μm]
0	0.00
5	16.30
10	32.58
15	48.85
20	65.15

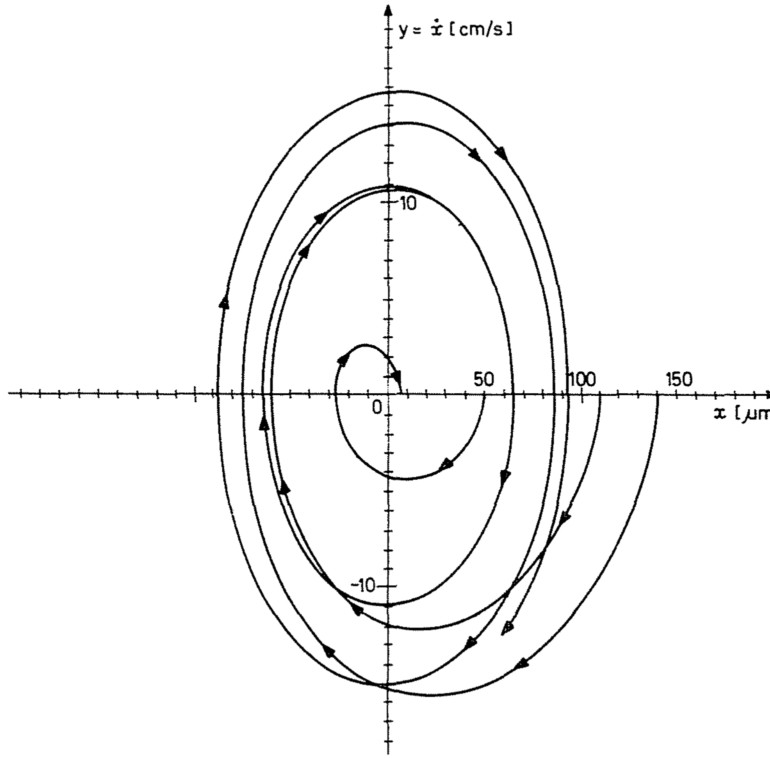

Fig. 11. Phase trajectories

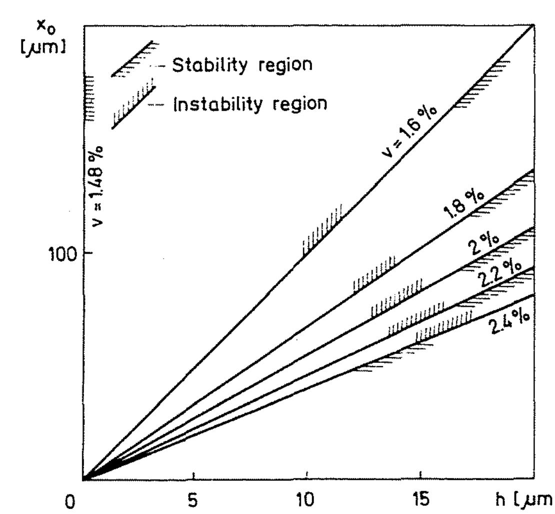

Fig. 12a. Relation between backlash and critical magnitude of the initial con. sig. $x_0(h)$

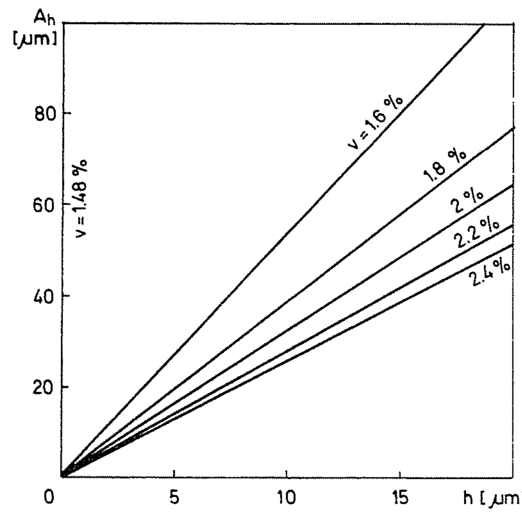

Fig. 12b. Relation between backlash and critical oscillation amplitude

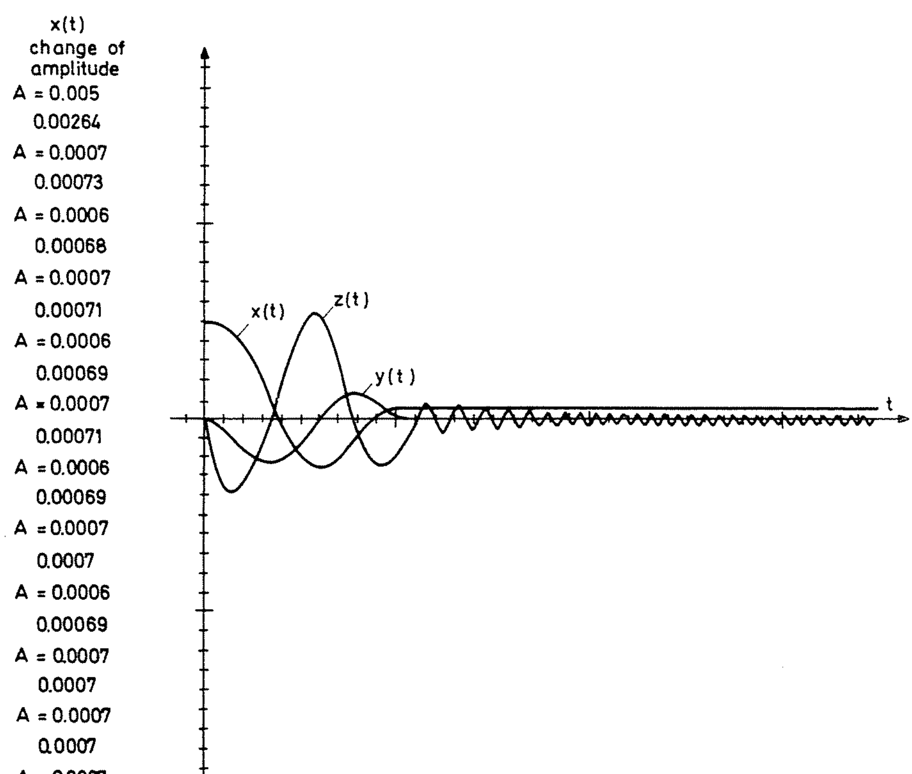

Fig. 13a. Case of stability (corresponding to Fig. 11)

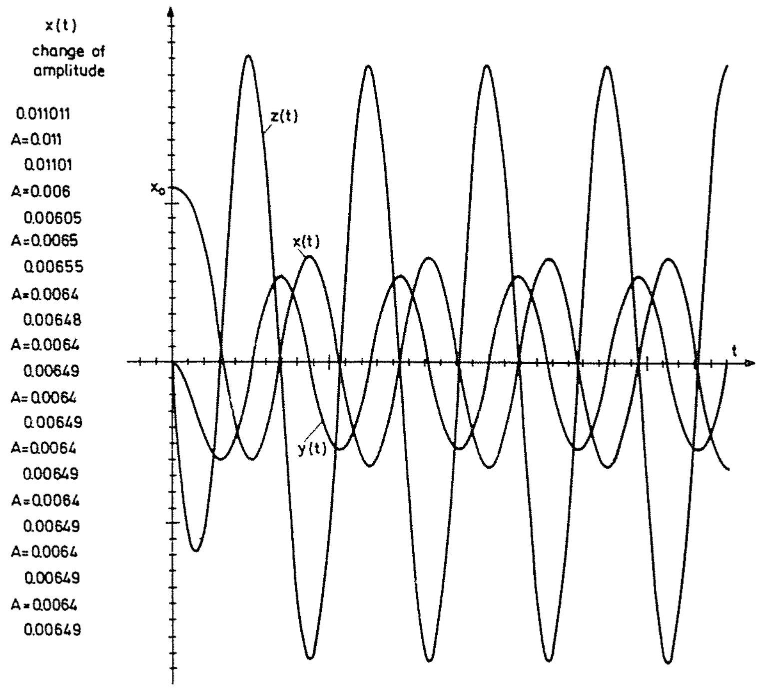

Fig. 13b. Case of stability limit (corresponding to Fig. 11)

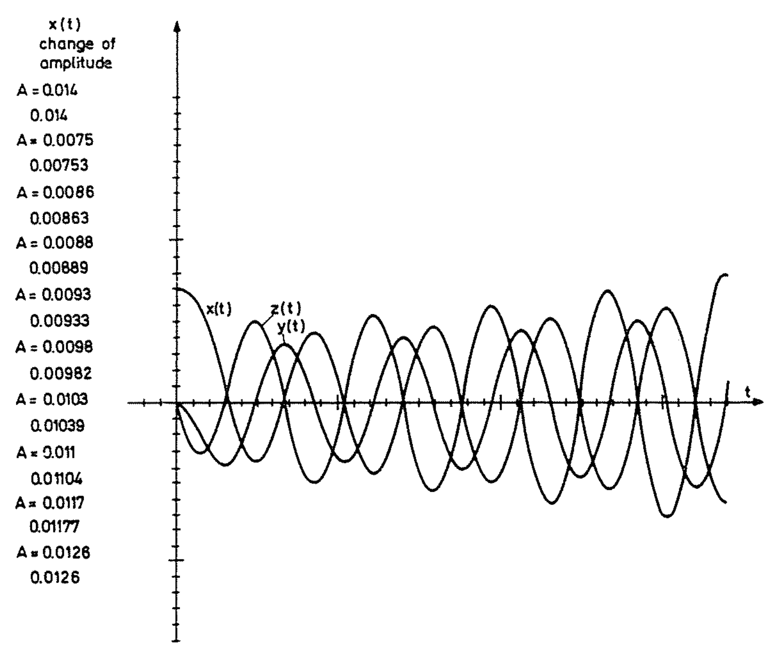

Fig. 13c. Case of instability (corresponding to Fig. 11)

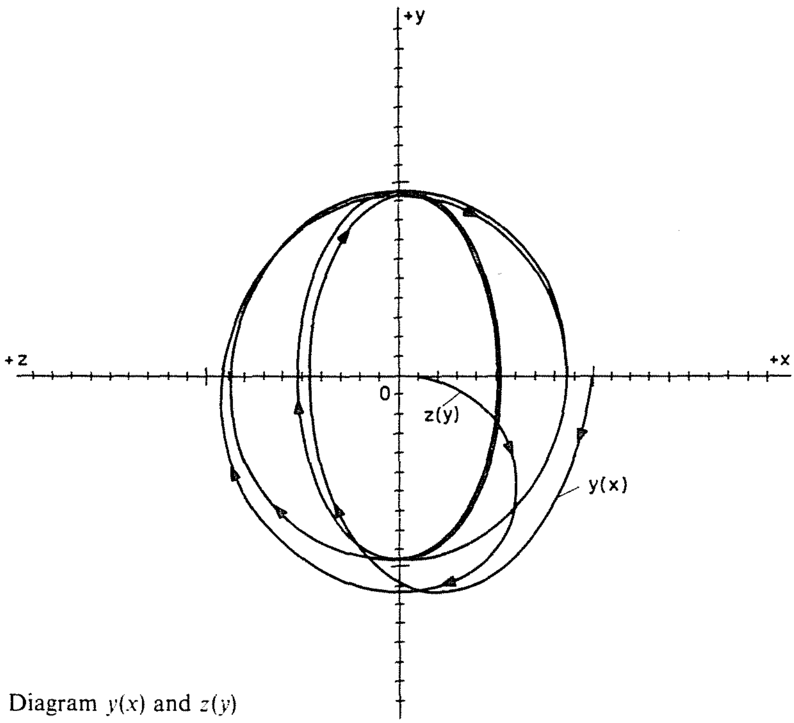

Fig. 14. Diagram $y(x)$ and $z(y)$

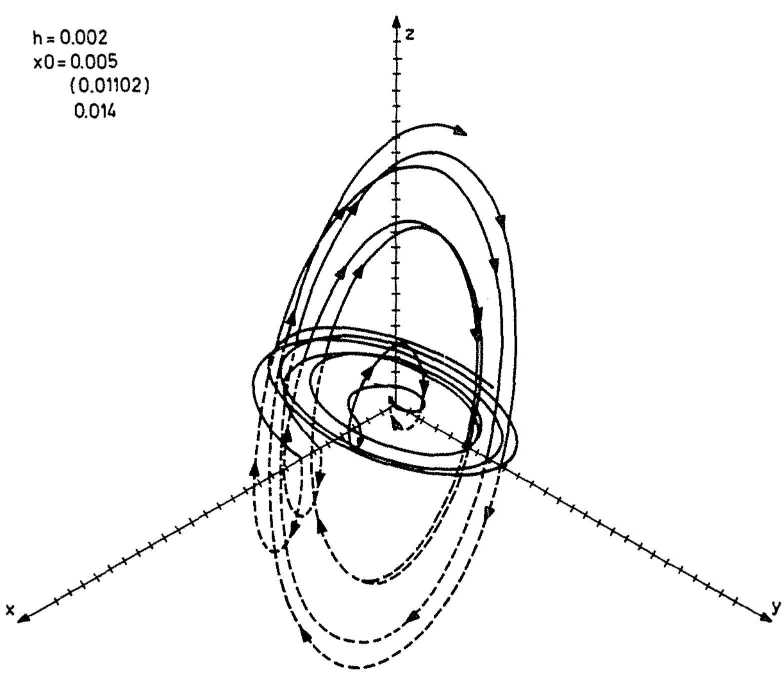

Fig. 15. Spatial trajectories (corresponding to Fig. 11)

Conclusions and discussion

On basis of the results obtained above we may state the following:

1. If the hydraulic fluid compressibility is negligible (i.e., the incompressible case) and there is a hysteresis backlash in the system, the limit cycle occurs. This result corresponds completely to the one received by the other method [1]. An interesting fact is that between backlash magnitude and limit cycle amplitude a linear relation exists. It suggests that in the presence of this type of nonlinearity, the original linear system still retains some of its linear property (see Fig. 11).

2. On the other hand, if the hydraulic fluid compressibility is not negligible, and its variation is also considered, the linear element of this system is a third-order one (its characteristic polynomial is third-order) and in the presence of hysteresis nonlinearity the system behavior totally differs from that of the second-order system. Namely:

a) In the system—using the terminology of the stability investigation of the nonlinear system—the limit cycle does not occur! It behaves as a conditional stable linear system considering the compressibility magnitude. In other words, at every magnitude of compressibility there is one and only one critical input signal. At every input of an amplitude smaller than the critical one, the system stays stable.

b) The hysteresis backlash ameliorates the stability property of the system in question, although it does so to the detriment of controlling accuracy. But in practice this situation is not always disavantageous because, for example, with a copying shaper when a roughing operation is made no one has to keep the magnitude smaller than a few micrometers. In the concrete example as the one above, when the mentioned volume ratio v of magnitude is 2%, the system is unstable. But if there is a backlash h of magnitude 20 μm the system steady-state is the vibration which has an amplitude of 65 μm (we are of course not considering how such a vibration damages the system, from the point of its life). Every initial controlled signal amplitude, with a magnitude smaller than 110 μm, there is no vibration in the system, and the controlled error in a steady-state takes a certain magnitude within the dead zone magnitude of 2h which is symmetrical to zero.

c) If the system is stable then the backlash cannot make it instable. This fact confirms once more the statement in point b). Consequently its situation differs from the one of the second-order system where the presence of the hysteresis backlash puts a stop to the nature of structural stability. In the second-order system the limit cycle is disadvantageous from the point of both the controlling accuracy and the mechanical stress due to vibration. In practice it may be unusable because of its dynamical quality.

The statements discussed above are supported by a physical fact, namely that in the third-order system the backlash, within certain limits, brakes the feedback effect, moreover it may put a stop to the feedback if the amplitude of the initial controlled signal is not greater than backlash h.

3. In the third-order system model if we consider the volume ratio of air-oil mixture as a system operation parameter, then between the initial magnitude of the controlled signal x_0 and backlash h, there exists a linear relation which divides the first quarter of plane (x_0, h) into two regions, one characterized by stability and the other by instability as shown in Fig. 13. Besides, an increase of the volume ratio v diminishes the stability region. The situation of the critical oscillation amplitude is similar (see Fig. 14).

Despite the preceding linear property, the system still retains an essential feature of nonlinearity, thus the system is stable for only the signals of small magnitudes. It is well known that from the viewpoint of stability the general property of all linear systems, their stability depends only upon the nature of the system, but does not depend upon the initial magnitude of the signal.

4. The common application of the phase-space and the numerical analysis method—especially when a convenient graphical computer program is used—makes an investigation of the problem evident and simple. Besides we can more easily and rapidly determine the occurrence of the limit cycle (in the second-order system) or the stability limit (in the third-order system). Because in phase-space both the limit cycle and the stability limit make a trajectory which tends towards a certain closed curve (a closed trajectory), all projections of this trajectory are also closed curves if we consider the simple curve piece as the degenerated case of the trajectory projections.

The phase-space method is not a new idea. But in the past its application was very rare due to the complications of computation and graphical technics. Modern computers put an end to these problems and so the phase-space method may become a good method for investigating engineering system dynamics.

Acknowledgement

The author wishes to thank Prof. Dr. Olivér Petrik, head of Department of Precision-Mechanics and Applied Optics, Technical University of Budapest for his careful revision of the paper and his support in publication.

References

1. CSÁKI, F.: Korszerű szabályozáselmélet. Akadémiai Kiadó, Budapest 1970 (Modern control theory. "Akadémiai" Publishing House, Budapest 1970)
2. BROOME, D. R.: The effect of load flexibility in hydraulic manipulator. Transaction of the Institute of Measurement and Control. Vol. 4, No 3, July-Sept 1982
3. LUGOSI, L.: Hidraulikus irányítástechnika. Müszaki Könyvkiadó, Budapest, 1968. (Hydraulic steering technics "Műszaki" Publishing House, Budapest, 1968)
4. TRAN VAN DAC: The effect of hydraulic fluid modulus variation due to air bubbles in hydraulic positional servomechanisms Periodica Polytechnica: Mechanical Engineering. Technical University of Budapest (BME) (in press)

TRAN VAN DAC H-1521 Budapest